

**Stimulated emission of surface plasmon polaritons by lead-sulphide quantum dots at near infra-red wavelengths**

Radko, Ilya P.; Nielsen, Michael Grøndahl; Albrektsen, Ole; Bozhevolnyi, Sergey I.

*Published in:*  
Optics Express

*DOI:*  
[10.1364/OE.18.018633](https://doi.org/10.1364/OE.18.018633)

*Publication date:*  
2010

*Document version*  
Final published version

*Citation for published version (APA):*

Radko, I. P., Nielsen, M. G., Albrektsen, O., & Bozhevolnyi, S. I. (2010). Stimulated emission of surface plasmon polaritons by lead-sulphide quantum dots at near infra-red wavelengths. *Optics Express*, 18(18), 18633-18641. <https://doi.org/10.1364/OE.18.018633>

**Terms of use**

This work is brought to you by the University of Southern Denmark through the SDU Research Portal. Unless otherwise specified it has been shared according to the terms for self-archiving. If no other license is stated, these terms apply:

- You may download this work for personal use only.
- You may not further distribute the material or use it for any profit-making activity or commercial gain
- You may freely distribute the URL identifying this open access version

If you believe that this document breaches copyright please contact us providing details and we will investigate your claim. Please direct all enquiries to [puresupport@bib.sdu.dk](mailto:puresupport@bib.sdu.dk)

# Stimulated emission of surface plasmon polaritons by lead-sulphide quantum dots at near infra-red wavelengths

I. P. Radko,\* M. G. Nielsen, O. Albrektsen, and S. I. Bozhevolnyi

*Institute of Sensors, Signals, and Electrotechnics (SENSE), University of Southern Denmark,  
Niels Bohrs Allé 1, DK-5230 Odense M, Denmark*

[\\*ilr@sense.sdu.dk](mailto:*ilr@sense.sdu.dk)

**Abstract:** Amplification of surface plasmon polaritons in planar metal-dielectric structure through stimulated emission is investigated using leakage-radiation microscopy configuration. The gain medium is a thin polymethylmethacrylate layer doped with lead-sulphide nanocrystals emitting at near-infrared wavelengths. We demonstrate an optical gain of  $\sim 200 \text{ cm}^{-1}$  for the mode under consideration, which corresponds to  $\sim 32\%$  compensation of SPP loss.

© 2010 Optical Society of America

**OCIS codes:** (240.6680) Surface plasmons; (250.4480) Optical amplifiers; (250.5403) Plasmonics; (230.3120) Integrated optics devices.

---

## References and links

1. S. A. Maier, *Plasmonics: Fundamentals and applications* (Springer, 2007).
2. S. Lal, S. Link and N. J. Halas, "Nano-optics from sensing to waveguiding," *Nature Photon.* **1**, 641–648 (2007).
3. J. N. Anker, W. P. Hall, O. Lyandres, N. C. Shah, J. Zhao and R. P. Van Duyne, "Biosensing with plasmonic nanosensors," *Nature Mater.* **7**, 442–453 (2008).
4. D. K. Gramotnev and S. I. Bozhevolnyi, "Plasmonics beyond the diffraction limit," *Nature Photon.* **4**, 83–91 (2010).
5. D. J. Bergman and M. I. Stockman, "Surface plasmon amplification by stimulated emission of radiation: quantum generation of coherent surface plasmons in nanosystems," *Phys. Rev. Lett.* **90**, 027402 (2003).
6. J. Seidel, S. Grafström, and L. Eng, "Stimulated emission of surface plasmons at the interface between a silver film and an optically pumped dye solution," *Phys. Rev. Lett.* **94**, 177401 (2005).
7. M. A. Noginov, V. A. Podolskiy, G. Zhu, M. Mayy, M. Bahoura, J. A. Adegoke, B. A. Ritzo, and K. Reynolds, "Compensation of loss in propagating surface plasmons polariton by gain in adjacent dielectric medium," *Opt. Express* **16**, 1385–1392 (2008).
8. M. A. Noginov, G. Zhu, M. Mayy, B. A. Ritzo, N. Noginova, and V. A. Podolskiy, "Stimulated emission of surface plasmon polaritons," *Phys. Rev. Lett.* **101**, 226806 (2008).
9. M. A. Noginov, G. Zhu, A. M. Belgrave, R. Bakker, V. M. Shalaev, E. E. Narimanov, S. Stout, E. Herz, T. Suteewong, and U. Wiesner, "Demonstration of a spaser-based nanolaser," *Nature (London)* **460**, 1110–1113 (2009).
10. I. De Leon and P. Berini, "Amplification of long-range surface plasmons by a dipolar gain medium," *Nature Photon.* **4**, 382–387 (2010).
11. M. Ambati, S. H. Nam, E. Ulin-Avila, D. A. Genov, G. Bartal, and X. Zhang, "Observation of stimulated emission of surface plasmon polaritons," *Nano Lett.* **8**, 3998–4001 (2008).
12. J. Grandidier, G. Colas des Francs, S. Massenet, A. Bouhelier, L. Markey, J.-C. Weeber, C. Finot, and A. Dereux, "Gain-assisted propagation in a plasmonic waveguide at telecom wavelength," *Nano Lett.* **9**, 2935–2939 (2009).
13. I. P. Radko, S. I. Bozhevolnyi, G. Brucoli, L. Martín-Moreno, F. J. García-Vidal, and A. Boltasseva, "Efficient unidirectional ridge excitation of surface plasmons," *Opt. Express* **17**, 7228–7232 (2009).
14. I. P. Radko, S. I. Bozhevolnyi, G. Brucoli, L. Martín-Moreno, F. J. García-Vidal, and A. Boltasseva, "Efficiency of local surface plasmon polariton excitation on ridges," *Phys. Rev. B* **78**, 115115 (2008).
15. I. De Leon and P. Berini, "Theory of surface plasmon-polariton amplification in planar structures incorporating dipolar gain media," *Phys. Rev. B* **78**, 161401(R) (2008).

16. I. De Leon and P. Berini, "Modeling surface plasmon-polariton gain in planar metallic structures," *Opt. Express* **17**, 20191–20202 (2009).
17. A. L. Stepanov, J. R. Krenn, H. Ditlbacher, A. Hohenau, A. Drezet, B. Steinberger, A. Leitner, and F. R. Aussenegg, "Quantitative analysis of surface plasmon interaction with silver nanoparticles," *Opt. Lett.* **30**, 1524–1526 (2005).
18. A. Drezet, A. Hohenau, D. Koller, A. Stepanov, H. Ditlbacher, B. Steinberger, F. R. Aussenegg, A. Leitner, and J. R. Krenn, "Leakage radiation microscopy of surface plasmon polaritons," *Mater. Sci. Eng. B* **149**, 220–229 (2008).
19. H. Raether, *Surface plasmons on smooth and rough surfaces and on gratings* (Springer, 1988).
20. T. Holmgaard and S. I. Bozhevolnyi, "Theoretical analysis of dielectric-loaded surface plasmon-polariton waveguides," *Phys. Rev. B* **75**, 245405 (2007).
21. M. Kerker, *The scattering of light and other electromagnetic radiation* (Academic Press, 1969).
22. P. M. Bolger, W. Dickson, A. V. Krasavin, L. Liebscher, S. G. Hickey, D. V. Skryabin, and A. V. Zayats, "Amplified spontaneous emission of surface plasmon polaritons and limitations on the increase of their propagation length," *Opt. Lett.* **35**, 1197–1199 (2010).
23. J. Gosciniaik, S. I. Bozhevolnyi, T. B. Andersen, V. S. Volkov, J. Kjelstrup-Hansen, L. Markey, and A. Dereux, "Thermo-optic control of dielectric-loaded plasmonic waveguide components," *Opt. Express* **18**, 1207–1216 (2010).
24. E. Kretschmann, "The determination of the optical constants of metals by excitation of surface plasmons," *Z. Physik* **241**, 313–324 (1971).
25. A. Bouhelier and G. P. Wiederrecht, "Excitation of broadband surface plasmon polaritons: Plasmonic continuum spectroscopy," *Phys. Rev. B* **71**, 195406 (2005).
26. T. Søndergaard and S. I. Bozhevolnyi, "Theoretical analysis of finite-size surface plasmon polariton band-gap structures," *Phys. Rev. B* **71**, 125429 (2005).

## 1. Introduction

Plasmonics is a rapidly growing area of nano-optics utilizing localized and propagating resonance oscillations of free electrons in metallic nanostructures. The great interest to plasmonics is explained by a large set of applications ranging from telecommunications and signal processing to biochemistry and sensing [1–4]. Yet, there is a fundamental constraint that hinders the full implementation of plasmonic devices — ohmic loss resulting in relatively quick power dissipation in metal. Amplification of plasmonic modes using an active medium surrounding the metallic structure could be a solution to this problem [5]. Already quite a number of studies have demonstrated stimulated emission of surface plasmon polaritons (SPPs). Particularly, plasmon gain (or even complete compensation of SPP loss) has been achieved using optical pumping of dye molecules [6–10], erbium ions [11] or quantum dots (QDs) [12]. The latter work deals with lead-sulphide (PbS) nanocrystals emitting at telecommunication wavelengths. This paper reports on partial SPP loss compensation in planar structures incorporating a dielectric film doped with PbS QDs with fluorescence emission peak centred at a near-infrared wavelength.

## 2. Experimental configuration and methods

We investigate a four-layer structure composed of a quartz substrate, a 50-nm-thick gold film, a thin layer of polymethylmethacrylate (PMMA, molecular weight  $MW = 350K$ , prepared by spin-coating of a  $\sim 1.5$  weight percent solution in toluene) with embedded PbS QDs, and air (Fig. 1a). The gold-PMMA interface supports at least one (pure plasmonic) mode, which is excited through vertical illumination of a periodic set of gold ridges with a tightly focused continuous-waveform (CW) laser beam (diameter  $d \sim 5.8 \mu\text{m}$  at the  $1/e^2$  level of intensity) at the wavelength of 860 nm. This SPP mode is to be amplified and hence it is referred to as probe SPP, whereas the corresponding laser beam used for its excitation is called probe laser beam. The geometry of ridges is adjusted for efficient unidirectional SPP excitation. We have thoroughly investigated a similar geometrical configuration (without a PMMA layer) previously [13] in terms of the possibility to locally excite SPP and found its ability to convert

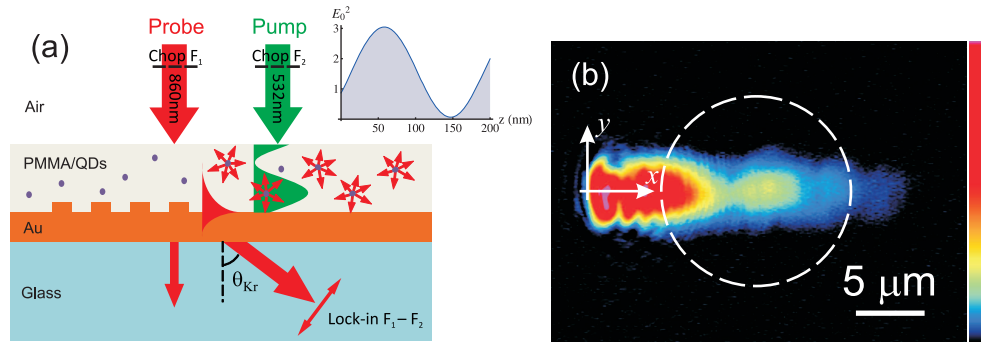


Fig. 1. (a) Experimental configuration. Thin PMMA film doped with PbS quantum dots on top of a 50-nm-thick gold film. Excitation of a probe SPP beam ( $\lambda = 860$  nm) is achieved through a grating. Inset shows a calculated distribution of the intensity of the pump beam ( $\lambda = 532$  nm) inside the PMMA layer. (b) Leakage-radiation microscopy image of a probe SPP beam. The dashed circle shows the position where the pump beam is focused.

above  $\sim 40\%$  of the incident laser power into an SPP signal. Addition of a PMMA layer on top of the structure merely shifts the wavelength, at which the most efficient SPP excitation is expected [14], without changing the main observed characteristics of the system. We leverage this configuration here to provide strong probe-SPP power.

The lead-sulphide QDs (Evident Technologies, concentration in the PMMA layer  $N \sim 4.6 \times 10^{19} \text{ cm}^{-3}$ ) exhibit a fluorescence emission peak at 876 nm and were pumped at 532 nm with a CW laser beam focused into a spot with diameter  $d \sim 13.8 \mu\text{m}$  at the  $1/e^2$  level of intensity (Fig. 1b). Reflection of the gold-PMMA interface is close to minus unity, and consequently the field near the metal surface is rather small, which has obviously a negative effect on the maximum achievable gain [15, 16]. However, due to the interference of the incident beam with its reflection, the first constructive maximum occurs at a distance of  $\sim \lambda/(4n)$ , where  $\lambda = 532$  nm and  $n \approx 1.5$  (refractive index of PMMA), so that a considerable amount of pump energy is concentrated within the thin polymer layer (inset in Fig. 1a).

The probe SPP is detected by collecting the corresponding leakage radiation (LR) appearing at the quartz-substrate side of the sample at the Kretschmann angle,  $\theta_{\text{Kr}}$  [17, 18]. Importantly, the intensity of the LR is proportional to the intensity of the probe SPP [19], making it possible to evaluate the amplification of the probe SPP mode. However, in order to detect the LR signal correctly, one must know the corresponding SPP-mode index. Using transfer-matrix approach for a multilayer structure we have calculated the SPP-mode index and propagation length versus the PMMA-film thickness for a free-space wavelength of 860 nm (Fig. 2). When the polymer-layer thickness is approaching the zero value, there is only one mode with the effective index and the propagation length corresponding to the mode of the gold film-air interface. With the increase of the PMMA-film thickness this mode tends towards that of the gold film-PMMA interface, and *s*- (pure photonic) and *p*-polarized (hybrid plasmonic) modes appear in an alternating sequence. The dispersion properties of such a four-layer structure are discussed in details elsewhere [20]. Note that only the first *p*-polarized mode is essential in our consideration, since the remaining modes exist merely by virtue of the choice of a particular experimental PMMA-layer thickness that is convenient for investigation. For this reason, we kept the polymer thickness below 350 nm (cut-off thickness for the second *p*-polarized mode) and used a polarizer to eliminate the signal from the first *s*-polarized mode in the detected LR (Fig. 2). Additionally, we applied a narrow band-pass interference filter (centred at 860 nm, full width at half-maximum is 10 nm) upon detection to suppress background from the pump beam.

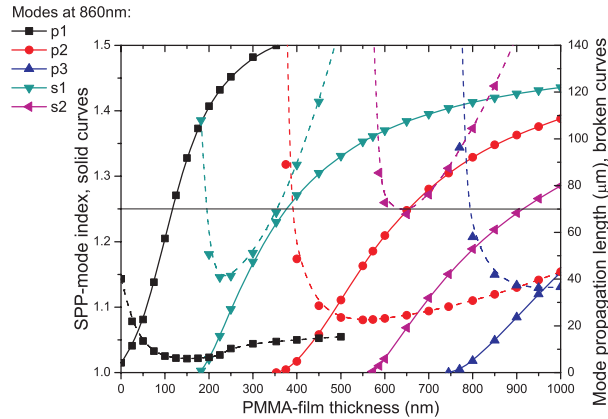


Fig. 2. Calculated effective mode index (solid curves) and mode propagation length (broken curves) for the first three  $p$ -polarized hybrid plasmonic modes (p1, p2, p3) and the first two  $s$ -polarized photonic modes (s1, s2) existing in a four-layer structure: air/PMMA/50-nm-gold/glass.

We note also that our LR microscopy setup (similar to that described in [17]) contains an objective with numerical aperture  $NA = 1.25$ . Hence, only those modes whose guide index is below that value can be directly observed (the configuration space below the horizontal line in Fig. 2). Others might be detected only as light scattered inside the objective.

There are three contributions into the detected LR at 860 nm: (i) The main part of the signal stems from the original (unamplified) probe SPP; (ii) another component is from spontaneous emission of the QDs leading to both light tunnelled through the gold film and to an (incoherent with the probe SPP) excitation of plasmons; (iii) finally, the third component is from stimulated emission of the QDs also contributing with light tunnelling through the gold film and, in this case, plasmons excited coherently with the probe SPP. In order to quantify the value of stimulated emission and the corresponding gain of the probe SPP, we measure separately two of the three contributions into the LR (i and iii). This is done by exploiting a modulation scheme with phase-sensitive detection (lock-in amplification). The probe SPP is modulated at  $f_1 = 280$  Hz by mechanically chopping the laser beam that is used for its excitation. The pump laser beam is chopped with the same (double-frequency) wheel at  $f_2 = 200$  Hz (Fig. 1a). Hence, the contribution of the probe SPP into the LR is detected by a lock-in amplifier with the reference frequency being  $f_1 = 280$  Hz, whereas the contribution from stimulated emission is provided by setting the reference to either the sum or the difference of the frequencies  $f_1$  and  $f_2$ ; we used 80 Hz in our experiment.

We should note that since we pump an area covering only partially the probe SPP beam, gain occurs at a limited distance of SPP travelling. From the experimental perspective, this means that the relative increase of the LR signal due to stimulated emission of SPP [i.e., the ratio of component (iii) to (i)] does not show the actual SPP gain, which would be the case only if the whole sample were pumped homogeneously. Instead, the stimulated emission is collected from a confined area, and hence recalculation into the actual SPP gain is required. The appendix to this article is devoted to derivation of the corresponding analytical expression and also introduces a so called leakage coefficient, which might be found useful for the LR microscopy of SPP in general.

### 3. Results and discussions

Preliminary study of the possibility to obtain stimulated emission of SPP showed that the effect is relatively weak and substantial amount of probe and pump power is required. This, however, can lead to gradual melting of a very thin PMMA layer and change the described mode distribution (Fig. 2) in the structure. We found the reliable range of incident powers by measuring the LR from the probe SPP versus the power of the probe laser beam in the absence of pump signal (Fig. 3a). This dependence must be linear and the slope of the curve shows the SPP excitation efficiency [13]. This was indeed observed for probe laser powers below 35–40 mW. With the further increase of the power the dependence first becomes superlinear, which is explained by a decrease of the PMMA-film thickness with subsequent increase of the mode propagation length (see Fig. 2) and reduced overall QD absorption. An even further increase of the probe laser power leads to saturation probably due to damaging of the ridge configuration as the intensity of the local field near the ridges is an order of magnitude higher than that of the incident field [13].

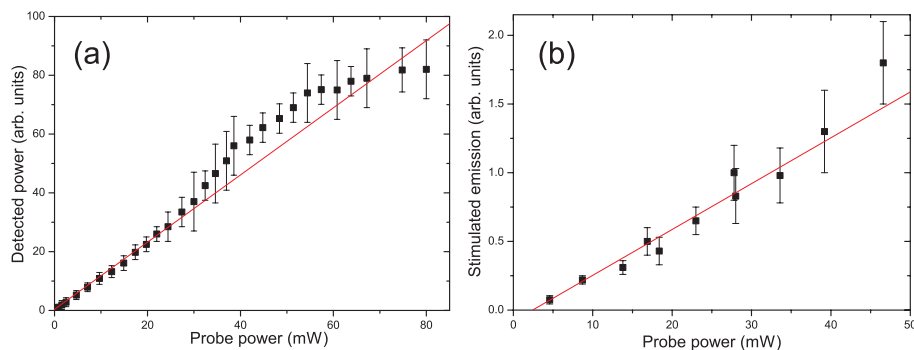


Fig. 3. (a) Detected optical signal versus the probe power in the absence of pump irradiance (pure SPP excitation). The red line is a guide for the eyes and shows the linear range for the probe power. (b) Measured value of stimulated emission signal of the first (pure plasmonic) *p*-polarized mode versus the probe power in the four-layer structure with the PMMA-film thickness being  $(85 \pm 15)$  nm. The pump power is constant and set to 13 mW. The pump line in panel (b) is a linear fit to the data points.

The process of stimulated emission of SPP is investigated by measuring its value (more precisely, its contribution into LR) versus the probe and the pump irradiance with one of these two parameters being fixed. First, the pump power is set at a moderate value of 13 mW and the probe-laser power is varied. The dependence obtained is close to linear (Fig. 3b). Knowing the probe-SPP mode loss and the value of overlap between the probe SPP and the pump beam (Fig. 1b) allows evaluating [Appendix, Eq. (11)] the SPP-mode gain from the SPP stimulated emission vs. probe power dependence. The gain appears to be nearly constant within the measured power range and features only a slight increase with the increasing probe-laser power (Fig. 4a). This indicates that the measurements are done in a saturation regime when available excited states of the QDs are nearly exhausted.

It is possible to raise the saturation level by increasing the pump power, and hereby provide more excited states of the QDs available for stimulated emission. Thus measurement with a fixed probe-laser power (18.3 mW) and a variable pump power yields gain of  $(205 \pm 30)$   $\text{cm}^{-1}$  at the maximum available irradiance, after which the PMMA layer starts to deteriorate and results in a decreased stimulated emission (Fig. 4b). According to Fig. 2, the SPP-mode propagation length for an 85-nm-thick PMMA layer is  $\sim 8$   $\mu\text{m}$ , which corresponds to an SPP-mode

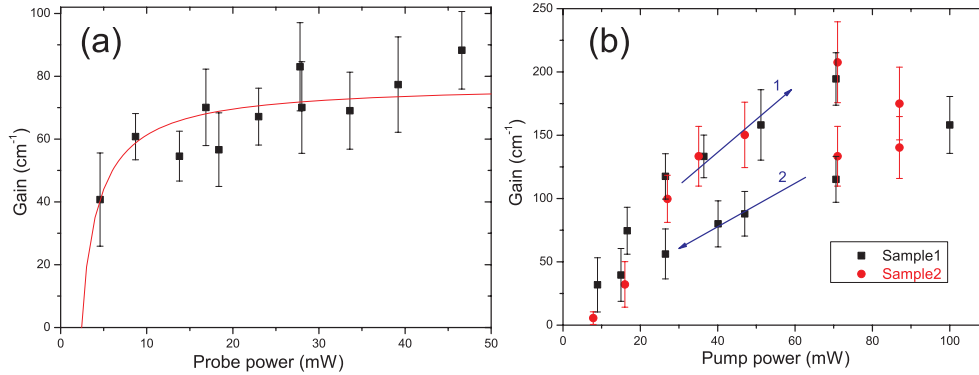


Fig. 4. (a) Evaluated [using data shown in Fig. 3b and Eq. (11) of Appendix] optical gain of the first (pure plasmonic)  $p$ -polarized mode versus the probe power in the four-layer structure with the PMMA-film thickness being  $(85 \pm 15)$  nm. The pump power is constant and set to 13 mW. The red curve is a phenomenological dependence obtained in assumption of linear signal growth in Figs. 3a and 3b. (b) Optical gain [same configuration, measured and evaluated in the same way as in panel (a)] versus the pump power while the probe power is fixed at 18.3 mW. Arrows 1 and 2 show the sequence of measurements and therefore indicate QD photo-bleaching as well as destruction of the PMMA layer at high pump power.

loss of  $625 \text{ cm}^{-1}$  or  $\sim 32\%$  of SPP-loss compensation for the achieved gain. However, one must keep in mind that QDs embedded in the PMMA layer absorb at the probe wavelength too, decreasing hereby the SPP propagation length. The effect can be estimated by introducing an effective imaginary part of the dielectric permittivity of the polymer,  $\epsilon''$ , using the following expression (see, e.g., [21]):

$$\epsilon'' = \frac{\sqrt{\epsilon} \lambda}{2\pi} N \sigma_{\text{abs}}. \quad (1)$$

Here  $\epsilon$  is the (real) dielectric constant of PMMA,  $\lambda$  is the free-space wavelength,  $N$  is the concentration of those QDs (in the PMMA) that absorb at the wavelength  $\lambda$ , i.e. the concentration of the QDs residing in the ground state, and  $\sigma_{\text{abs}}$  is the QD absorption cross-section. From the producer of the QDs the latter quantity is stated to be  $\sigma_{\text{abs}} = 9.9 \times 10^{-17} \text{ cm}^2$  for a wavelength of 751 nm and can be recalculated for 860 nm using a measured absorption spectrum (not shown), which provides an absorbance — the value directly proportional to the absorption cross-section. We obtained  $\sigma_{\text{abs}} = 2.9 \times 10^{-17} \text{ cm}^2$  at  $\lambda = 860 \text{ nm}$ . Assuming all QDs to be in the ground state ( $N \sim 4.6 \times 10^{19} \text{ cm}^{-3}$ ), one gets  $\epsilon'' = 0.027$ , from which the SPP-mode propagation length is evaluated as  $\sim 3.4 \mu\text{m}$ , i.e. more than twice shorter than that calculated (Fig. 2) without taking into account QD absorption. This value corresponds to the upper bound of the SPP-mode loss of  $\sim 1470 \text{ cm}^{-1}$  [note that relative to this value, the mode-loss compensation is still  $\sim 32\%$  according to Eq. (11) of Appendix], which must be substantially overestimated, since the number of QDs residing in the ground state is reduced at least twice in the case of population inversion.

The dependence shown in Fig. 4b is not expected to be linear, since the used probe power of 18.3 mW might fall into an interval of gain saturation or fast growth of gain (Fig. 4a) depending on the pump power, which shifts the saturation level. Moreover, the dependence of the gain on the pump irradiance should also exhibit saturation behaviour because of the effect of amplified spontaneous emission [22]. Yet the latter was not clearly observed perhaps due to the relatively high probe-SPP intensity as compared with the values given in [22] and due to the

destruction of the PMMA layer. High probe irradiance increases the probability of stimulated emission effectively suppressing the spontaneous decay channel. However, such suppression is only possible in experiments where the probe power can be directly adjusted. This would normally require either to increase the signal that is to be amplified anyway, which is obviously not possible, or to increase the Q-factor of a SPP resonator (SPASER), which might be undesirable.

#### 4. Conclusion

In summary, we have studied the possibility of SPP-loss compensation at near-infrared wavelengths using gain medium incorporating lead-sulphide quantum dots. By exploiting a configuration for efficient SPP excitation [13], we achieve a relatively high probe signal, decreasing hereby the probability of spontaneous emission. We demonstrate moderate SPP gain of  $\sim 200 \text{ cm}^{-1}$ , which can nevertheless be comparable to intrinsic SPP-mode loss if an optimum configuration is chosen. For instance, the SPP-mode at an interface between two semi-infinite gold-PMMA media has a propagation length of  $\sim 18 \mu\text{m}$  at the investigated wavelength, which is equivalent to SPP-mode loss of  $\sim 270 \text{ cm}^{-1}$ . On the other hand, the choice of our experimental system is dictated by the necessity to detect and evaluate the stimulated emission of SPPs, for which a leakage-radiation microscopy setup is selected. This imposes a limitation on the maximum metal-film and gain-medium thicknesses for the leakage radiation detection to be possible, and therefore introduces additional losses to the SPP mode under investigation. Use of a thin polymer film together with a pump beam illuminating the QDs from the air side also decreases gain effect because of the non-uniform pump distribution and enhanced non-radiative transitions of the QDs close to the metal surface [15, 16]. If a thin metal film is employed, pumping can be realized by illumination in the Kretschmann configuration, which should substantially increase the overlap between the probe and the pump fields. Finally, addition of a dielectric layer on top of the metal structure leads unavoidably to SPP mode damping even in the absence of the dielectric absorbance (see mode propagation length on Fig. 2). However, this layer is indispensable for realization of waveguiding [20] or various types of active functionality such as, for instance, thermo-optic modulation [23]. We therefore leverage the unavoidable presence of this dielectric medium by introducing gain into the system. Use of a low-index dielectric, such as CYTOP, as a matrix medium for QDs should increase the SPP propagation length making complete compensation of intrinsic SPP loss more feasible.

#### 5. Appendix: Evaluation of SPP-mode gain from LR microscopy measurements

Since our estimation of the value of SPP-mode gain by QDs is based on LR microscopy measurements, we are aimed at deriving an expression that relates the magnitude of the measured LR signal with the corresponding gain of the SPP mode.

*Leakage coefficient* Let us define a leakage coefficient  $\tau$  as a relative amount of SPP power being elastically radiated into the substrate in the form of LR, i.e.,

$$P_{\text{LR}} = \tau P_{\text{SPP}}, \quad (2)$$

where  $P_{\text{LR}}$  is the power of LR and  $P_{\text{SPP}}$  is the total power guided by the SPP beam. Assuming a plane SPP wave and denoting SPP electric-field attenuation along the propagation direction  $x$  due to internal loss (ohmic and, if present, absorption loss in the dielectric medium, for instance, due to QDs) by  $\alpha$  and attenuation due to radiation loss by  $\beta$ , the amplitude of the SPP field at the metal surface can be written as  $E(x) = E_0 e^{-\alpha x} e^{-\beta x}$ . We can also introduce gain  $\gamma$  into the system by writing  $E(x) = E_0 \cdot \exp[-(\alpha + \beta + \gamma)x]$ . Hence, the power transferred by the SPP beam through a plane  $x = \text{const}$  is expressed as follows:

$$P(x) = P_{\text{SPP}} \cdot \exp[-2(\alpha + \beta + \gamma)x]. \quad (3)$$

This formula assumes that the SPP emerges at the plane  $x = 0$  and its total power (at the origin) is  $P_{\text{SPP}}$ . The value of  $\beta$  depends on the metal-film thickness  $d$ , and for an infinitely thick film it is equal to zero. By definition, the SPP propagation length  $L_{\text{SPP}}(d) = 1/[2(\alpha + \beta + \gamma)]$ . Denoting  $l = L_{\text{SPP}}(d = d_0)$  and  $L = L_{\text{SPP}}(d = \infty)$ , we get  $l/L = (\alpha + \gamma)/(\alpha + \beta + \gamma)$ , and hence:

$$\frac{\beta}{\alpha + \beta + \gamma} = 1 - \frac{l}{L}. \quad (4)$$

We then note that SPP-power loss solely due to LR is equal, with the minus sign, to the SPP power radiated into the substrate from an interval  $dx$ , i.e. from Eq. (3),

$$\frac{dP_{\text{LR}}}{dx} = - \left. \frac{dP}{dx} \right|_{\substack{\alpha=0 \\ \gamma=0}} = 2\beta P(x). \quad (5)$$

Integration of this expression from 0 to  $+\infty$  gives  $P_{\text{LR}} = P_{\text{SPP}} \cdot \beta / (\alpha + \beta + \gamma)$ , and hence from Eqs. (2) and (4) we finally get:

$$\tau = \frac{\beta}{\alpha + \beta + \gamma} = \frac{L - l}{L}. \quad (6)$$

Equation (6) can be used to evaluate the leakage coefficient if SPP propagation length is known (for instance, from numerical simulations) for both cases: along a thin ( $l$ ) and an infinitely thick ( $L$ ) metal films. Analytical estimation of  $\tau$  using approximate expressions for  $\alpha$  and  $\beta$  [24, 25] also provides quite accurate values for visible, near-infrared and telecom wavelengths. In the absence of active medium, gain  $\gamma$  should be set to zero, i.e.,

$$\tau' = \frac{\beta}{\alpha + \beta}. \quad (6a)$$

Note that  $\tau > \tau'$ , since gain  $\gamma$  must be of opposite to  $(\alpha + \beta)$  sign. That means that the presence of gain effectively increases the leakage of SPP power into the substrate.

*Overlap between the SPP and the pump beams.* LR is collected from the whole visible surface imaged with an objective, whereas we pump an area covering only partially the probe SPP beam (Fig. 1b). For this reason, gain occurs at a limited distance of SPP travelling, and for quantitative estimates we will need to calculate the relative part of SPP power,  $P_{\text{circ}}$ , dissipated inside a circular surface area, where pumping is produced. This is done by calculating an overlap integral between the pump Gaussian beam and the probe SPP beam:

$$P_{\text{circ}} = \iint \frac{\partial^2 P(x,y)}{\partial x \partial y} \exp \left[ -2 \frac{(x-x_0)^2 + y^2}{R^2} \right] dx dy, \quad (7)$$

where  $(x_0, 0)$  and  $R$  are the position coordinate and the radius (waist) of the pump beam (Fig. 1b), and  $P(x, y)$  is the SPP power transferred through the point  $(x, y)$  of the surface. Expression for the derivative of  $P(x, y)$  can be found by noticing that  $(\partial/\partial y)P(x, y) = \int_{-\infty}^{+\infty} \langle S_x(x, y) \rangle_t dz$  with a time-averaged  $x$ -component of the SPP Poynting vector under the integral:  $\langle S_x(x, y) \rangle_t = \frac{c}{8\pi} E_z \text{Re}[H_y]$ . The latter can be analytically calculated using an expression for the field of an SPP Gaussian beam (Eq. (2) in [26]). Comparing the calculated value of  $P_{\text{circ}}$  with the total power of SPP beam,  $P_{\text{SPP}} = \iint \partial^2 P(x, y) / \partial x \partial y \cdot dx dy$ , gives the desired value:

$$k = P_{\text{circ}} / P_{\text{SPP}}. \quad (8)$$

For the experimental parameters,  $x_0 = (10 \pm 0.5) \mu\text{m}$  and  $R = (6.9 \pm 0.4) \mu\text{m}$ , we obtained  $k = (0.201 \pm 0.025)$ , i.e.  $\sim (20 \pm 3)\%$  of the probe-SPP power is dissipated inside the dashed circle

in Fig. 1b (note a highly nonlinear colour scale, which visually enhances the SPP propagation length).

*SPP-mode gain.* In the experiment on SPP amplification, the LR signal has a component corresponding to the probe-SPP beam and a component corresponding to stimulated emission from the QDs. The enhanced LR signal (as compared with the case of unamplified SPP) can be accounted for as either an additional stimulated SPP emission emerging (coherently with the probe SPP) inside the circular area (Fig. 1b) and leaking into the substrate with the leakage coefficient  $\tau'$ , Eq. (6a), when the gain is effectively absent, or as a probe-SPP power leaking from the circular area with an increased leakage coefficient  $\tau$ , Eq. (6), due to the presence of gain in the system [see also a note after Eq. (6a)]. Mathematically this can be expressed as follows:

$$(P_{\text{circ}} + P_{\text{st}}) \tau' = P_{\text{circ}} \tau, \quad (9)$$

where  $P_{\text{st}}$  is the total power of stimulated SPP emission and  $P_{\text{circ}}$  is given by Eq. (8). On the other hand, by virtue of the definition of the leakage coefficient and on the strength of Eq. (8),

$$\begin{aligned} P_{\text{st}} &= M_{\text{st}}/\tau', \\ P_{\text{circ}} &= kP_{\text{SPP}} = kM_{\text{SPP}}/\tau', \end{aligned} \quad (10)$$

with  $M_{\text{st}}$  and  $M_{\text{SPP}}$  being the measured values of stimulated SPP emission and the total SPP power detected at reference frequencies  $f_1 - f_2 = 80$  Hz and  $f_1 = 280$  Hz, respectively. Combining Eqs. (6), (6a), (9), and (10), we finally get an expression for gain  $\gamma$  involving the experimentally measured values:

$$\gamma = -(\alpha + \beta) \frac{M_{\text{st}}}{M_{\text{st}} + kM_{\text{SPP}}}. \quad (11)$$

The value of  $(\alpha + \beta)$  is evaluated from the SPP propagation length as  $1/(2L_{\text{SPP}})$ .

### Acknowledgments

This work was supported by the Danish Council for Independent Research (FTP contract No. 09-072949). The authors cordially thank Alexey V. Krasavin for useful discussions.